



Dual strands of the *miR-223* duplex (*miR-223-5p* and *miR-223-3p*) inhibit cancer cell aggressiveness: targeted genes are involved in bladder cancer pathogenesis

Sho Sugawara^{1,2} · Yasutaka Yamada^{1,2} · Takayuki Arai^{1,2} · Atsushi Okato^{1,2} · Tetsuya Idichi³ · Mayuko Kato^{1,2} · Keiichi Koshizuka¹ · Tomohiko Ichikawa² · Naohiko Seki¹

Received: 11 February 2018 / Revised: 18 February 2018 / Accepted: 20 February 2018 / Published online: 14 March 2018

© The Author(s) under exclusive licence to The Japan Society of Human Genetics 2018

Abstract

Analyses of microRNA (miRNA) expression signatures obtained by RNA sequencing revealed that some passenger miRNAs (*miR-144-5p*, *miR-145-3p*, *miR-149-3p*, *miR-150-3p*, and *miR-199a-3p*) acted as anti-tumor miRNAs in several types of cancer cells. The involvement of passenger strands in the pathogenesis of human cancer is a novel concept. Based on the miRNA signature of bladder cancer (BC) obtained by RNA sequencing, we focused on both strands of the *miR-223*-duplex (*miR-223-5p* and *miR-223-3p*) and investigated their functional significance in BC cells. Ectopic expression of these miRNAs showed that both *miR-223-3p* (the guide strand) and *miR-223-5p* (the passenger strand) inhibited cancer cell migration and invasion of BC cells. The role of *miR-223-5p* (the passenger strand) has not been well studied. Combining gene expression studies and in silico database analyses, we demonstrated the presence of 20 putative target genes that could be regulated by *miR-223-5p* in BC cells. Among these targets, high expression of five genes (*ANLN*, *INHBA*, *OIP5*, *CCNB1*, and *CDCA2*) was significantly associated with poor prognosis of BC patients based on The Cancer Genome Atlas (TCGA) database. Moreover, we showed that a gene (*ANLN*) encoding a multifunctional actin-binding protein was directly regulated by *miR-223-5p* in BC cells. Overexpression of *ANLN* was observed in BC clinical specimens and high expression of *ANLN* was significantly associated with poor prognosis of BC patients. We suggest that studies of regulatory cancer networks, including the passenger strands of miRNAs, may provide new insights into the pathogenic mechanisms of BC.

Introduction

Bladder cancer (BC) is a commonly diagnosed urologic cancer that constitutes the ninth most common cause of cancer-related death worldwide [1]. In 2015, it was

estimated that ~76,000 new cases of BC were diagnosed and 1600 patients died in the United States of America [2]. Approximately 70–80% of patients are categorized with non-muscle-invasive BC (NMIBC) at the first diagnosis and high relapse rates (50–70%) are observed in patients with NMIBC [3, 4]. Unfortunately, more than 15% of recurrent BC patients develop muscle-invasive BC (MIBC); the 5-year survival rate for patients with MIBC is approximately 60% [5]. At present, there are no effective therapeutic strategies for patients with lymph node and distant metastasis or failure of first-line treatment [6]. Therefore, elucidation of the molecular pathogenesis underlying the acquisition of MIBC phenotypes and identification of therapeutic targets are urgent issues that must be addressed to improve the poor prognosis of BC patients.

MicroRNAs (miRNAs) belong to a group of small non-coding RNA molecules that act as pivotal agents responsible for fine-tuning RNA expression in a sequence-dependent manner [7, 8]. The unique nature of miRNA is that a single miRNA species might control the expression of

Electronic supplementary material The online version of this article (<https://doi.org/10.1038/s10038-018-0437-8>) contains supplementary material, which is available to authorized users.

✉ Naohiko Seki
naoseki@faculty.chiba-u.jp

¹ Department of Functional Genomics, Chiba University Graduate School of Medicine, Chiba, Japan

² Department of Urology, Chiba University Graduate School of Medicine, Chiba, Japan

³ Department of Digestive Surgery, Breast and Thyroid Surgery, Graduate School of Medical Sciences, Kagoshima University, Kagoshima, Japan

a large number of protein-coding (or noncoding) genes in normal or diseased cells [9]. Thus, abnormal expression of miRNAs can disrupt RNA networks and can lead to human diseases [10–15]. There is substantial evidence that dysregulated miRNAs are deeply involved in the development of cancer cells, as well as their metastasis and drug resistance [11–16]. We have been analyzing anti-tumor miRNAs in BC based on miRNA signatures to clarify their contribution to BC pathogenesis [17–19].

The general concept of miRNA biogenesis posits that the passenger strand of miRNA (the minor strand or miRNA*) derived from duplex miRNA is degraded and does not regulate gene expression [20, 21]. Contrary to this theory, construction of miRNA signatures by RNA sequencing revealed that some miRNA passenger strands (*miR-144-5p*, *miR-145-3p*, *miR-149-3p*, *miR-150-3p*, and *miR-199a-3p*) were downregulated in several cancers compared with normal tissues [17, 22–24]. Our previous studies of BC revealed that *miR-144-5p* and *miR-139-3p* possessed anti-tumor roles through targeting of *CCNE1/2* and *MMP11*, respectively [18, 25]. These facts have changed the concept of miRNA biogenesis and demonstrated the importance of analyzing miRNA passenger strands in cancer.

In this study, we focused on both strands of the *miR-223* duplex, i.e., *miR-223-5p*, the passenger strand and *miR-223-3p*, the guide strand. We used miRNA signatures to investigate their anti-tumor roles and determine the relevant oncogenic networks in BC cells. We suggest that identification of novel function of passenger strands of miRNAs and the RNA networks they regulate might enhance our understanding of the molecular pathogenesis of BC.

Materials and methods

Human tissue samples and BC cell lines

Clinical tissue samples (BC and normal tissues) were collected from patients who underwent total cystectomy or nephroureterectomy at Chiba University Hospital between 2014 to 2015. The characteristics of the patients with BC are summarized in Supplemental Table 1. Written informed consent was obtained from all patients who were told the outline of the study and the use of the samples for scientific research. The protocol of this study was approved by the Institutional Review Board of Chiba University; approval number is 484.

In this study, we used two human BC cell lines, BOY and T24. The BOY cell line was established at Kagoshima University and was derived from a male Asian patient. The T24 cell line was obtained from the American Type Culture Collection. Details of the two cell lines were described previously [26, 27].

Transfection of mature miRNAs and small interfering RNAs

The following molecular reagents were used for functional assays: mature miRNAs, mature miRNA precursors (*hsa-miR-223-5p*, assay ID: PM 12672; *hsa-miR-223-3p*, assay ID: PM 12301; Applied Biosystems, Foster City, CA, USA), miRNA control (assay ID: AM 17111; Applied Biosystems), and small interfering RNA (siRNA) (Stealth Select RNAi siRNA; si-*ANLN* P/N: HSS122893 and HSS182497; Invitrogen, Carlsbad, CA, USA). The procedures for transfecting these small RNAs into cancer cell lines have been described [26, 27].

Quantitative real-time reverse transcription polymerase chain reaction

To measure the expression of *miR-223-5p*, *miR-223-3p*, and *ANLN* in normal tissues, cancer tissues and cell lines, the following procedures and reagents were used. For quantitative real-time reverse transcription polymerase chain reaction (qRT-PCR), we utilized P/N: 002098 (Applied Biosystems) for *miR-223-5p* and P/N: 002295 for *miR-223-3p*. To assess *ANLN*, we used an assay-on-demand gene expression product (P/N: Hs01122612_m1; Thermo Fisher Scientific). To normalize the data, we used human *GUSB* (P/N: Hs99999908_m1; Applied Biosystems), *GAPDH* (P/N: Hs02758991_m1; Applied Biosystems) and *RNU48* (assay ID: 001006; Applied Biosystems). The qRT-PCR procedures were described earlier [26, 27].

Functional assays for cell proliferation, migration, and invasion

The procedures for assessment of cell proliferation, migration and invasion have been described [26, 27].

Preparation of the miRNA-incorporated fraction by Ago2 immunoprecipitation

We investigated whether the passenger strand of miRNA (*miR-223-5p*) was actually incorporated into the RNA-induced silencing complex (RISC). Immunoprecipitation was carried out using a human Ago2 miRNA isolation kit (Wako, Osaka, Japan) in order to purify miRNA-incorporated fractions after *miR-223-5p* or *miR-223-3p* transfection. The procedure was carried out according to the manufacturer's protocol [28].

Western blot and immunohistochemistry analysis

Antibodies used in this experiment were mouse monoclonal anti-*ANLN* antibodies (1:750 dilution; AMAb90662; Atlas

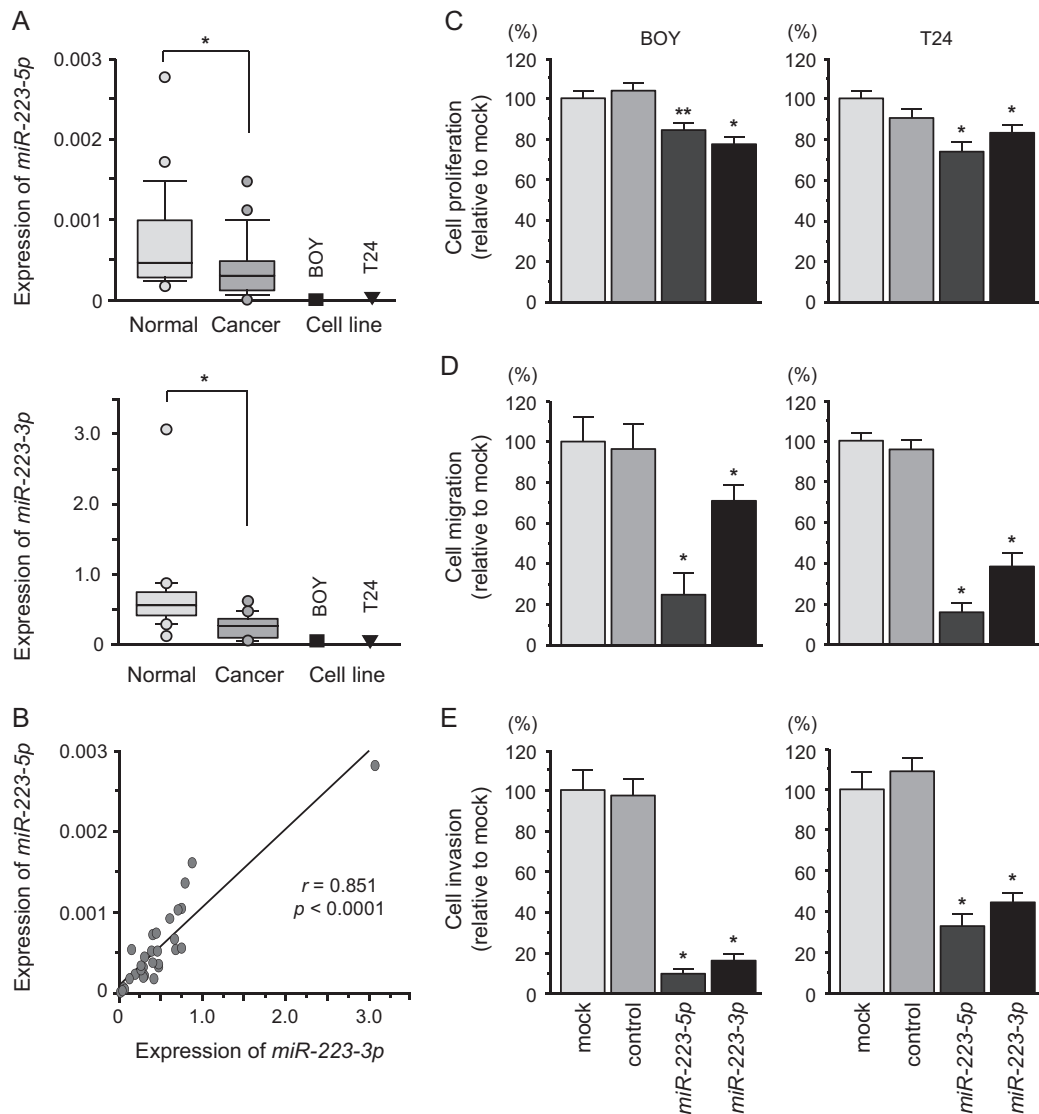


Fig. 1 Expression levels of *miR-223-5p* and *miR-223-3p* in BC clinical specimens and cell lines: functional analyses of those miRNAs in BC cells. **a** Quantitative real-time RT-PCR showed that the expression levels of *miR-223-5p* and *miR-223-3p* were significantly lower in BC tissues than in normal bladder tissues. Expression in two BC cell lines, BOY and T24, was lower than in normal bladder tissues. *RNU48* was used as an internal control. **b** Correlations among the relative

expression levels of *miR-223-5p* and *miR-223-3p*. **c–e** Effects of restoration of *miR-223-5p* and *miR-223-3p* in BC cells. Cell proliferation (72 h after transfection with 10 nM miRNA) and migration and invasion (48 h after transfection with 10 nM miRNA) were characterized after transfection with *miR-223-5p* or *miR-223-3p*. *, $P < 0.0001$; **, $P = 0.001$

Antibodies AB, Stockholm, Sweden). Anti-glyceraldehyde 3-phosphate dehydrogenase (GAPDH) antibodies (1:10,000 dilution; ab8245; Abcam, Cambridge, UK) were used as an internal control. The procedures for western blot analysis were described previously [26, 27].

Tissue samples were incubated overnight at 4 °C with anti-ANLN antibodies diluted 1:50 (AMAb90662; Atlas Antibodies AB) and anti-Ki67 antibodies diluted 1:50 (sc-15402; Santa Cruz Biotechnology, Santa Cruz, CA, USA). The procedure for immunohistochemistry was described previously [26, 27].

Identification of the putative oncogenic targets of *miR-223-5p* or *miR-223-3p* in BC cells

Oncogenic genes specifically affected by *miR-223-5p* or *miR-223-3p* in BC cells were identified by using a combination of in silico database and genome-wide gene expression analyses. TargetScan database (release 7.1) was used for prediction of putative targets of these miRNAs. Upregulated genes in BC clinical specimens were analyzed in Gene Expression Omnibus (GEO) data sets (accession numbers GSE 31684 and GSE 11783). Our original gene

expression data for *miR-223-5p*- or *miR-223-3p*-transfected cells were deposited in GEO database (accession number GSE 107008). Strategies for identifying miRNA targeted genes were described previously [22, 29].

Dual-luciferase reporter assays and vector construction

The wild-type or deletion-type sequences targeted by *miR-223-5p* were inserted in the psiCHECK-2 vector (C8021; Promega, Madison, WI, USA). After co-transfecting *miR-223-5p* and the constructed vector in T24 cells, firefly and *Renilla* luciferase activities were measured. *Renilla* luciferase intensity (*Renilla*/firefly) was expressed as normalized data. The procedure for dual-luciferase reporter assays was described in our previous studies [26, 27].

The Cancer Genome Atlas database analysis of BC samples

To investigate the clinical significance of the expression status of *ANLN* in BC patients, we analyzed The Cancer Genome Atlas (TCGA) datasets (The Cancer Genome Atlas: <https://tcga-data.nci.nih.gov/tcga/>). A large amount of cohort data was retrieved from cBioPortal (<http://www.cbioportal.org/>) and OncoLnc (data downloaded on 1 November 2017). Detailed information on the method is described in previous papers [26, 27].

Statistical analysis

The relationships between twogroups were analyzed using Mann–Whitney *U* tests. The relationships between three variables and numerical values were analyzed using Bonferroni-adjusted Mann–Whitney *U* tests. Spearman's rank tests were used to evaluate the correlation between the expression of *miR-223-5p* and *miR-223-3p*. Data analyses were performed using Expert StatView software, version 5.0 (Cary, NC, USA). Overall survival and disease-free survival of patients were estimated using the Kaplan–Meier method and log-rank tests with JMP PRO software (version 13; SAS Institute Inc., Cary, NC, USA).

Results

Expression levels of *miR-223-5p* and *miR-223-3p* in BC clinical specimens and cell lines

We evaluated the expression levels of *miR-223-5p* and *miR-223-3p* in 15 paired BC tissues and their matched adjacent non-cancer tissues. The results showed that the expression levels of *miR-223-5p* and *miR-223-3p* were significantly

lower in BC tissues than in adjacent noncancerous epithelium ($P < 0.0001$; Fig. 1a). In BOY and T24 cells, the expression of *miR-223-5p* and *miR-223-3p* was somewhat lower than non-cancerous clinical specimens (Fig. 1a).

In clinical specimens, a positive correlation between the expression levels of *miR-223-5p* and *miR-223-3p* was found by Spearman's rank test ($P < 0.0001$; Fig. 1b).

Investigation of the anti-tumor roles of *miR-223-5p* and *miR-223-3p* in BC cells

To evaluate the anti-tumor roles of both strands of the *miR-223*-duplex (*miR-223-5p* and *miR-223-3p*), we applied gain-of-function assays using mature miRNA restoration into two BC cell lines (BOY and T24).

Cancer cell proliferation was reduced by restoration of *miR-223-5p* and *miR-223-3p* in BC cells compared to mock- or miR-control-transfected cells (Fig. 1c). Likewise, cancer cell migration and invasion abilities were significantly suppressed by restoration of *miR-223-5p* and *miR-223-3p* in BC cells (Fig. 1d,e). These findings suggested that both strands of *miR-223-5p* and *miR-223-3p* acted as anti-tumor miRNAs in BC cells.

Incorporation of both strands of the *miR-223* duplex into RISC in BC cell

We investigated whether both strands of the *miR-223* duplex were actually functional in BC cells. The illustration of restored miRNAs incorporated into the RISC is shown in Supplemental Fig. 1. We carried out immunoprecipitation with antibodies targeting Ago2, which plays pivotal roles in the RISC. After mature miRNA transfection, we performed qRT-PCR to assess whether transfected miRNA was actually bound to Ago2. After transfection with *miR-223-5p* as a passenger strand and immunoprecipitation by anti-Ago2 antibodies, *miR-223-5p* levels were significantly higher than those of mock- or miR-control-transfected cells and those of *miR-223-3p*-transfected T24 cells ($P < 0.0001$; Supplemental Fig. 1).

Regulation of putative oncogenic targets by *miR-223-5p* and *miR-223-3p* in BC cells

Our strategy for identifying target oncogenes of *miR-223-5p* and *miR-223-3p* is shown in Supplemental Fig. 2. First, putative target genes of *miR-223-5p* were identified using the TargetScan database, leading us to 3164 genes. Next, we carried out genome-wide gene expression analysis using a microarray comparing *miR-223-5p*-transfected and mock-transfected T24 cells (accession number: GSE 107008). As a result, a total of 2556 genes were downregulated (\log_2 ratio < 0). Among these genes, we searched for genes that

Table 1 Candidate target genes regulated by *miR-223-5p* and *miR-223-3p* in BC

| (A) <i>miR-223-5p</i> | | | | | | |
|-----------------------|-----------------|---|--|-----------------------|-------------------------|----------------------------------|
| Entrez Gene ID | Gene symbol | Description | Downregulation of <i>miR-223-5p</i> transfected in T24 | Number of target site | GEO log ₂ FC | TCGA-OncoLnc Kaplan plot P-value |
| 83540 | <i>NUF2</i> | NUF2, NDC80 kinetochore complex component | -3.12 | 1 | 5.43 | 0.7700 |
| 23397 | <i>NCAPH</i> | Non-SMC condensin I complex, subunit H | -0.12 | 1 | 5.02 | 0.7950 |
| 54443 | <i>ANLN</i> | Anillin, actin binding protein | -1.90 | 1 | 4.54 | 0.0155 ^a |
| 4312 | <i>MMP1</i> | Matrix metalloproteinase 1 (interstitial collagenase) | -2.52 | 1 | 4.44 | 0.8340 |
| 8838 | <i>WISP3</i> | WNT1 inducible signaling pathway protein 3 | -0.34 | 1 | 4.39 | 0.1620 |
| 3624 | <i>INHBA</i> | Inhibin, beta A | -0.94 | 4 | 4.36 | 0.042 ^a |
| 8287 | <i>USP9Y</i> | Ubiquitin-specific peptidase 9, Y-linked | -0.43 | 1 | 3.94 | 0.3760 |
| 147841 | <i>SPC24</i> | SPC24, NDC80 kinetochore complex component | -1.49 | 1 | 3.92 | 0.2130 |
| 7546 | <i>ZIC2</i> | Zic family member 2 | -0.11 | 1 | 3.62 | 0.0617 |
| 11339 | <i>OIP5</i> | Opa interacting protein 5 | -1.51 | 2 | 3.58 | 0.0185 ^a |
| 6374 | <i>CXCL5</i> | Chemokine (C-X-C motif) ligand 5 | -0.93 | 1 | 3.57 | 0.4910 |
| 11130 | <i>ZWINT</i> | ZW10 interacting kinetochore protein | -2.58 | 1 | 3.48 | 0.9210 |
| 9837 | <i>GINS1</i> | GINS complex subunit 1 (Psf1 homolog) | -2.22 | 2 | 3.22 | 0.9500 |
| 79801 | <i>SHCBP1</i> | SHC SH2-domain binding protein 1 | -3.05 | 1 | 3.20 | 0.9180 |
| 9768 | <i>KIAA0101</i> | KIAA0101 | -1.56 | 1 | 3.18 | 0.6540 |
| 891 | <i>CCNB1</i> | Cyclin B1 | -1.59 | 1 | 3.12 | 0.0035 ^a |
| 157313 | <i>CDCA2</i> | Cell division cycle associated 2 | -1.98 | 1 | 3.12 | 0.0336 ^a |
| 8357 | <i>HIST1H3H</i> | Histone cluster 1, H3h | -1.21 | 1 | 3.09 | 0.6550 |
| 6913 | <i>TBX15</i> | T-box 15 | -1.02 | 3 | 3.05 | 0.7180 |
| 4085 | <i>MAD2L1</i> | MAD2 mitotic arrest-deficient-like 1 (yeast) | -1.89 | 2 | 3.03 | 0.7380 |
| (B) <i>miR-223-3p</i> | | | | | | |
| Entrez Gene ID | Gene symbol | Description | Downregulation of <i>miR-223-3p</i> transfected in T24 | Number of target site | GEO log ₂ FC | TCGA-OncoLnc Kaplan plot P-value |
| 6326 | <i>SCN2A</i> | Sodium channel, voltage gated, type II alpha subunit | -0.89 | 1 | 3.48 | 0.7310 |
| 25769 | <i>SLC24A2</i> | Solute carrier family 24 (sodium/potassium/calcium exchanger), member 2 | -0.94 | 1 | 3.47 | 0.5200 |
| 121355 | <i>GTSF1</i> | Gametocyte-specific factor 1 | -0.75 | 1 | 3.39 | 0.5140 |
| 115111 | <i>SLC26A7</i> | Solute carrier family 26 (anion exchanger), member 7 | -0.53 | 1 | 2.55 | — |
| 7545 | <i>ZIC1</i> | Zic family member 1 | -0.55 | 1 | 2.53 | 0.9960 |

Table 1 (continued)

| (B) <i>miR-223-3p</i> | | Downregulation of <i>miR-223-3p</i> | | TCGA-OncoLnc Kaplan | | |
|-----------------------|----------------|---|--------------------|-----------------------|-------------------------|----------------------|
| Entrez Gene ID | Gene symbol | Description | transfected in T24 | Number of target site | GEO log ₂ FC | plot <i>P</i> -value |
| 1894 | <i>ECT2</i> | Epithelial cell transforming 2 | -0.62 | 1 | 2.52 | 0.0281 ^a |
| 1869 | <i>E2F1</i> | E2F transcription factor 1 | -1.34 | 1 | 2.36 | 0.4350 |
| 10675 | <i>CSPG5</i> | Chondroitin sulfate proteoglycan 5 (neuroglycan C) | -0.55 | 1 | 2.34 | 0.6760 |
| 149018 | <i>LELP1</i> | Late cornified envelope-like proline-rich 1 | -1.70 | 1 | 2.33 | 0.9900 |
| 284403 | <i>WDR62</i> | WD repeat domain 62 | -1.27 | 1 | 2.15 | 0.7240 |
| 64137 | <i>ABCG4</i> | ATP-binding cassette, sub-family G (WHITE), member 4 | -0.59 | 1 | 1.85 | — |
| 2057 | <i>EPOR</i> | Erythropoietin receptor | -0.59 | 1 | 1.85 | — |
| 6602 | <i>SMARCD1</i> | SWI/SNF-related, matrix-associated, actin-dependent regulator of chromatin, subfamily d, member 1 | -0.03 | 1 | 1.81 | 0.7570 |
| 79838 | <i>TMC5</i> | Transmembrane channel-like 5 | -0.58 | 1 | 1.76 | 0.6120 |
| 374407 | <i>DNAJB13</i> | DnaJ (Hsp40) homolog, subfamily B, member 13 | -0.66 | 1 | 1.73 | 0.2850 |
| 6323 | <i>SCN1A</i> | Sodium channel, voltage gated, type I alpha subunit | -0.76 | 1 | 1.72 | 0.5620 |
| 6579 | <i>SLCO1A2</i> | Solute carrier organic anion transporter family, member 1A2 | -0.58 | 1 | 1.24 | 0.6460 |
| 403314 | <i>APOBEC4</i> | Apolipoprotein B mRNA editing enzyme, catalytic polypeptide-like 4 (putative) | -1.28 | 1 | 1.24 | 0.2480 |
| 23160 | <i>WDR43</i> | WD repeat domain 43 | -0.51 | 1 | 1.23 | — |
| 27173 | <i>SLC39A1</i> | Solute carrier family 39 (zinc transporter), member 1 | -0.87 | 1 | 1.15 | — |
| 388 | <i>RHOB</i> | ras homolog family member B | -0.53 | 1 | 1.14 | 0.00755 ^a |
| 24137 | <i>KIF4A</i> | Kinesin family member 4A | -1.56 | 1 | 1.13 | 0.0186 ^a |
| 81610 | <i>FAM83D</i> | Family with sequence similarity 83, member D | -0.51 | 1 | 1.06 | 0.109 |
| 5996 | <i>RGS1</i> | Regulator of G-protein signaling 1 | -0.28 | 1 | 1.03 | 0.261 |
| 6664 | <i>SOX11</i> | SRY (sex determining region Y)-box 11 | -1.21 | 1 | 1.01 | 0.314 |
| 5080 | <i>PAX6</i> | Paired box 6 | -1.27 | 1 | 1.01 | 0.27 |

^aPoor prognosis with a high expression

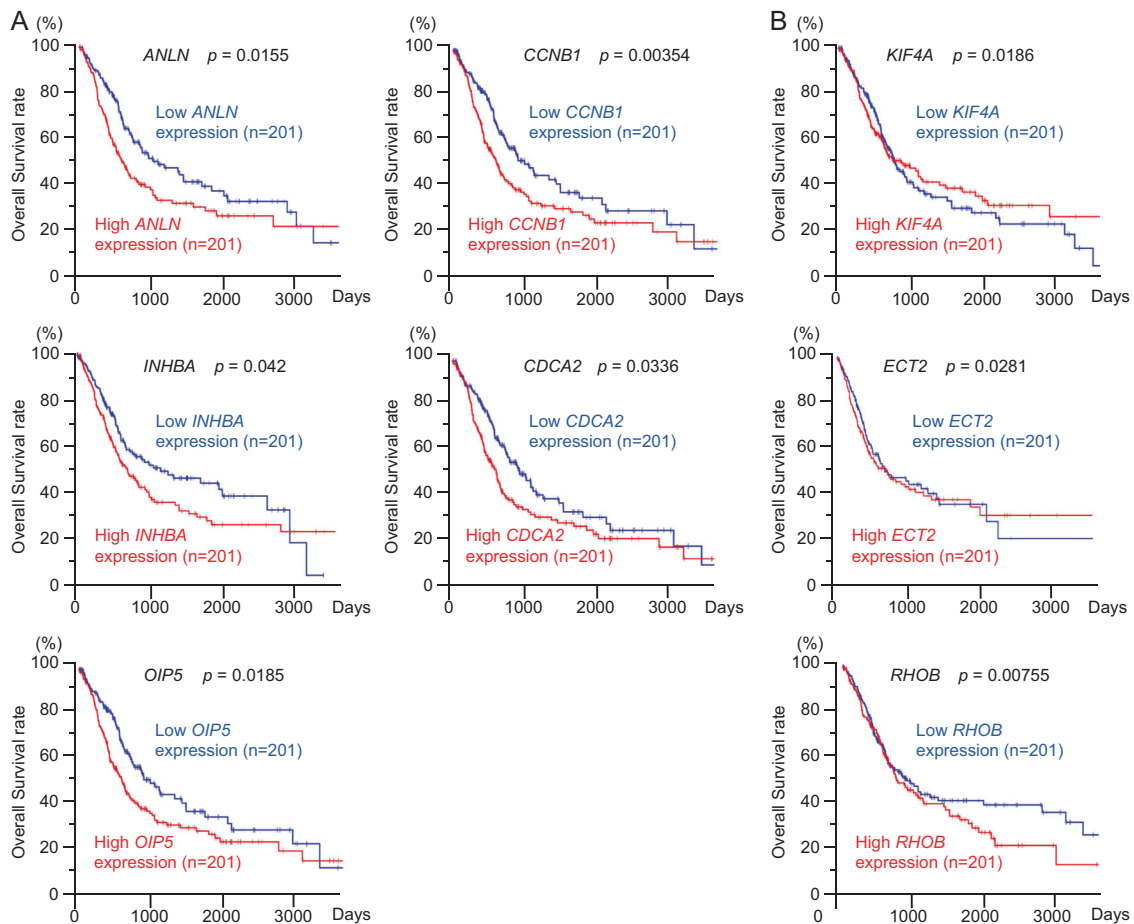


Fig. 2 Kaplan–Meier plots of overall survival vs. expression of the candidate genes regulated by *miR-223-5p* and *miR-223-3p* in BC cells. The Cancer Genome Atlas (TCGA) database was used to analyze

putative targets of *miR-223-5p* (a) and *miR-223-3p* (b) in BC. Kaplan–Meier plots of overall survival with log-rank tests for eight genes with high and low expression in the BC TCGA database

were upregulated in BC cells (\log_2 fold-change > 3), using publicly available gene expression data sets in GEO (accession number: GSE 31684 and GSE 11783). As a result, we identified 20 candidate target genes of *miR-223-5p* (Table 1A).

Using TCGA database, we investigated patient survival rates as a function of high- or low-expression levels of these genes. Among them, *CCNB1* had the greatest effect on overall survival, but *ANLN* was higher in GEO log fold-change data (Fig. 2a, b). Therefore, we focused on *ANLN* as a candidate gene of *miR-223-5p* (see below). Using a similar approach, we found that 26 genes were candidate targets of *miR-223-3p* regulation (Table 1B).

Direct regulation of *ANLN* by anti-tumor *miR-223-5p* in BC cells

We confirmed that gene expression of *ANLN* was significantly decreased in BC cells transfected with *miR-223-5p* compared to the mock or miR-control BC cell lines ($P < 0.001$; Fig. 3a). Western blotting analyses revealed that

ANLN protein levels of *miR-223-5p*-transfected BC cells were decreased compared to mock or miR-control BC cell lines (Fig. 3b). On the other hand, the expression of *ANLN* was not reduced in *miR-223-3p*-transfected BC cell lines at either the mRNA level or protein level (Fig. 3a, b).

Next, we performed luciferase reporter assays to determine whether *miR-223-5p* directly targeted the 3'-UTR region of *ANLN*. According to the TargetScan Human database, the binding site for *miR-223-5p* in the 3'-UTR of *ANLN* consisted of a single region (positions 1007–1013; Fig. 3c). We showed that *miR-223-5p* suppressed reporter activity of *ANLN* wild-type vector transfectants compared to mock or miR-control transfectants, whereas transfectants of the deletion-type vector were not decreased (Fig. 3d).

Effects of knockdown of *ANLN* in BC cells

To assess the effect of *ANLN* in BC cells, loss-of-function assays using siRNA were performed. We evaluated the knockdown efficiency of si-*ANLN*-transfected BC cell lines.

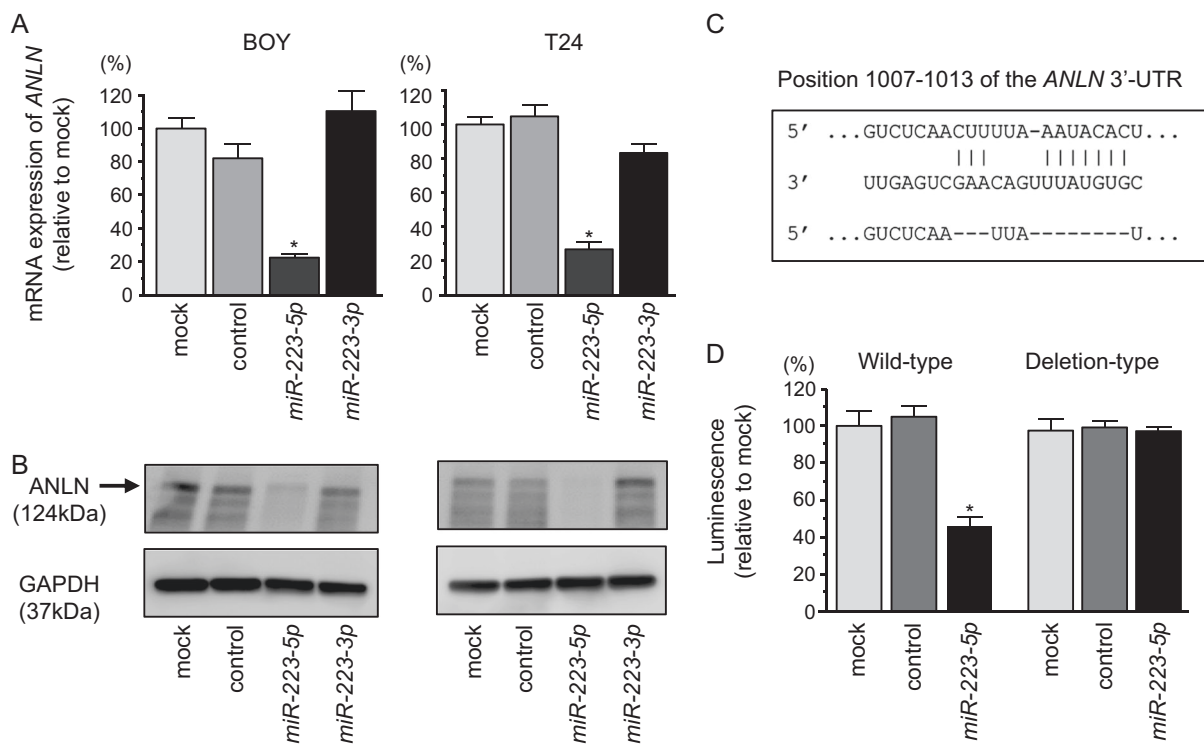


Fig. 3 Direct regulation of *ANLN* by *miR-223-5p* in BC cell lines. **a** *ANLN* mRNA expression in BC cell lines was evaluated by qRT-PCR 72 h after transfection with *miR-223-5p*. *GUSB* was used as an internal control. *, $P < 0.0001$. **b** *ANLN* protein expression in BC cell lines was evaluated by western blot analyses 72 h after transfection with *miR-223-5p*. GAPDH was used as a loading control. **c** *miR-223-5p*

binding sites in the 3'-UTR of *ANLN* mRNA. Dual luciferase reporter assays using vectors encoding putative *miR-223-5p* target sites (positions 1007-1013) of the *ANLN* 3'-UTR for both wild-type and deleted regions. Normalized data were calculated as ratios of *Renilla*/firefly luciferase activities. *, $P < 0.005$

Downregulation of *ANLN*/*ANLN* was detected in si-*ANLN* transfectants (Fig. 4a, b).

Cancer cell proliferation, migration, and invasion abilities were significantly blocked in si-*ANLN* transfectants compared to those in mock- or miR-control-transfected BC cell lines (Fig. 4c–e).

Expression of *ANLN*/*ANLN* in BC clinical specimens and its clinical significance

The mRNA levels of *ANLN* were upregulated in 15 BC tissues compared to adjacent noncancerous tissues ($P < 0.01$; Fig. 5a). To investigate the relationship between *ANLN* expression and clinical features, we searched the TCGA database. Kaplan–Meier analysis showed that the high *ANLN* expression group had a significantly lower disease-free survival compared to the low *ANLN* expression group ($P = 0.01$; Fig. 5b). The histologically poor grade group was higher in *ANLN* expression ($P < 0.0001$; Fig. 5c).

Finally, we carried out immunostaining analyses of clinical specimens to evaluate *ANLN* protein expression. Immunostaining analyses revealed that *ANLN* was more strongly expressed in the BC clinical specimens than in the non-cancer specimens. Notably, *ANLN* was expressed at

higher levels in the nuclei of the BC specimens. We also performed immunostaining of Ki67. The cells showing nuclear staining for *ANLN* were also positive for Ki67 (Fig. 5d). Therefore, it appeared that *ANLN* was expressed abundantly in the cancerous regions where cell proliferation was active.

Discussion

It is generally believed that only guide strands of miRNAs are incorporated into the RISC and control target gene expression [30]. Our original RNA sequencing-based miRNA expression signatures revealed that some passenger strands of miRNAs might be involved in cancer pathogenesis. This finding expands the number of miRNAs to be studied in cancer pathology research. For example, our recent studies showed that *miR-145-3p* (a passenger strand of the *miR-145*-duplex) had anti-tumor roles, as did *miR-145-5p* in several cancers [19, 23, 31, 32]. In prostate cancer (PCa), expression of anti-tumor *miR-145-3p* was significantly reduced in castration-resistant PCa specimens, and its targeted genes (*MELK*, *NCAPG*, *BUB1*, and *CDK1*) predicted survival in such patients [23]. More recently, we

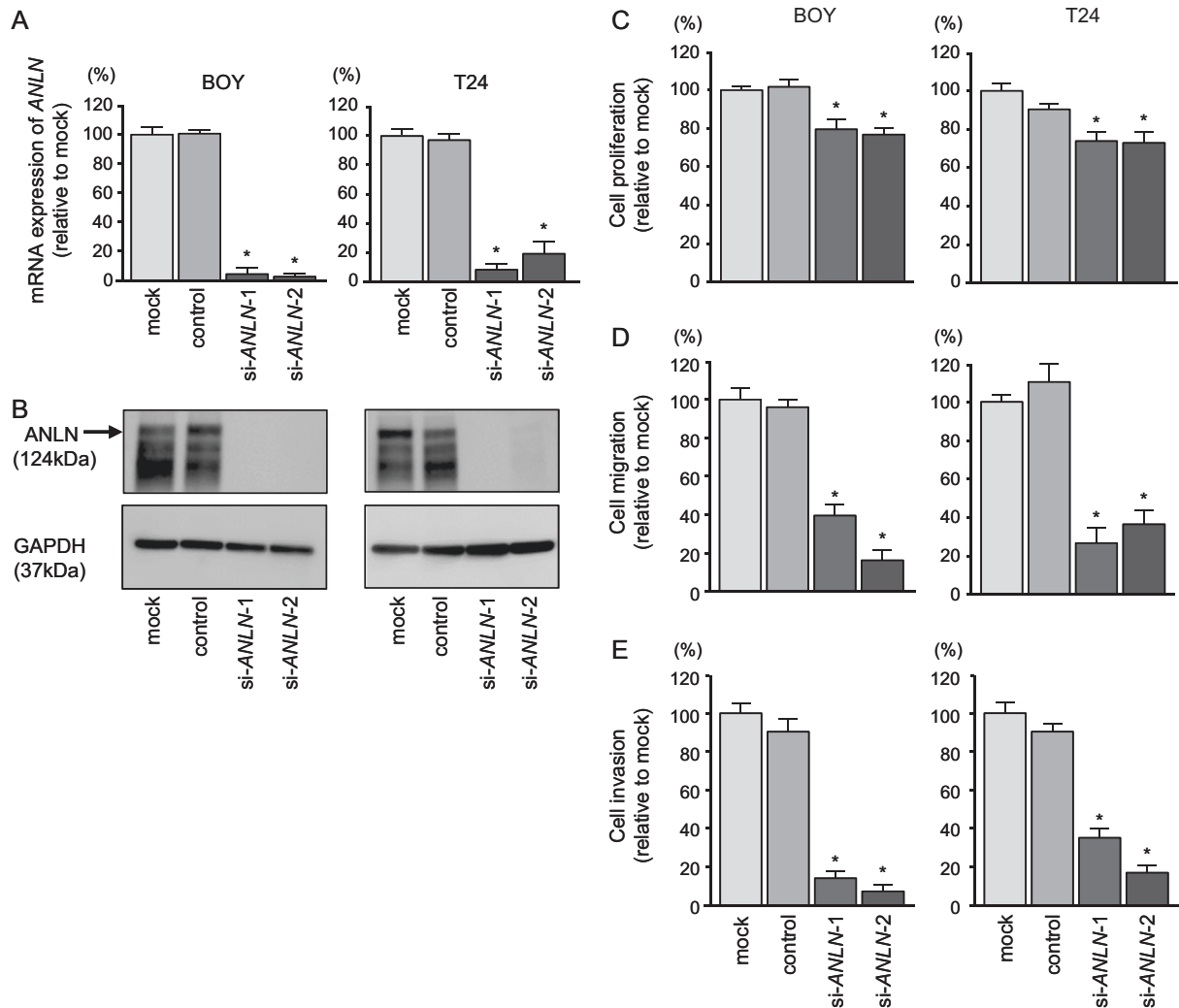


Fig. 4 Effects of *ANLN* silencing in BC cell lines. **a** *ANLN* mRNA expression in BC cell lines was evaluated by qRT-PCR 72 h after transfection with si-*ANLN*-1 or si-*ANLN*-2. *GUSB* was used as an internal control. **b** *ANLN* protein expression in BC cell lines was evaluated by western blot analysis 72 h after transfection with si-*ANLN*-1 or si-*ANLN*-2. GAPDH was used as a loading control. **c** Cell

proliferation was determined with the XTT assays 72 h after transfection with 10 nM si-*ANLN*-1 and si-*ANLN*-2. *, $P < 0.0001$. **d** Cell migration activity was determined by migration assays. *, $P < 0.0001$. **e** Cell invasion activity was determined using Matrigel invasion assays. *, $P < 0.0001$

confirmed that *miR-145-3p* possessed anti-tumor functions through its targeting of several oncogenes in head neck cancer [32].

Our present data showed that both strands of the *miR-223*-duplex (*miR-223-5p* and *miR-223-3p*) were down-regulated in BC tissues and that these miRNAs had anti-tumor roles. The anti-tumor functions of *miR-223-3p* (guide strand) were reported in several cancers, such as breast and cervical cancers [33, 34]. In contrast, oncogenic function of *miR-223-3p* was reported by several cancers, T-cell acute lymphoblastic leukemia and gastric cancer [35]. Our previous study of PCa showed that *miR-223-3p* was significantly reduced in naive PCa specimens and that ectopic expression of *miR-223-3p* significantly inhibited cancer cell migration and invasion [36]. Moreover, our study found that

expression of integrin $\alpha 3$ (*ITGA3*) and $\beta 1$ (*ITGB1*) was directly regulated by *miR-223-3p* in PCa cells [36]. Interestingly, both *ITGA3* and *ITGB1* were overexpressed in PCa tissues and knockdown of these integrins inhibited cancer cell aggressiveness through reduced downstream oncogenic signaling [36]. Strategies to block integrin-mediated oncogenic signaling might lead to new cancer treatments.

Previous studies showed that several transcription factors and oncogenes have been identified as *miR-223-3p* regulation in several cancer cell and disease cells [35, 37, 38]. In our present study of *miR-223-3p* target genes, some genes, e.g., *E2F1*, *SMARCD1*, *RHOB*, *SOX11*, and *PAX6*, have been reported as *miR-223-3p* regulation in previous reports [35, 37–42]. This indicates that our miRNA target search

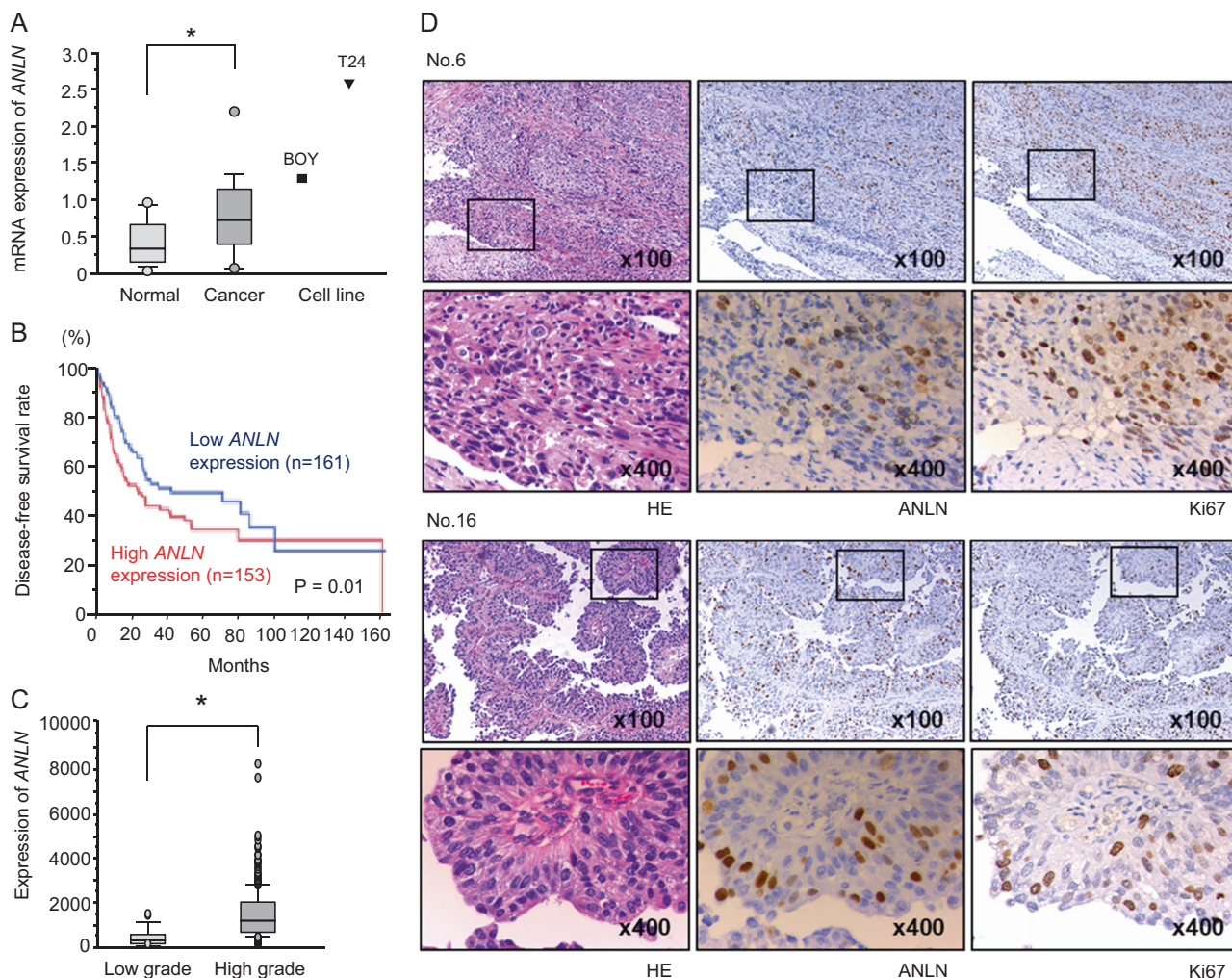


Fig. 5 Expression levels of *ANLN* mRNA and immunohistochemical staining of ANLN protein in BC specimens. **a** Expression levels of *ANLN* mRNA in BC or normal bladder tissues and BC cell lines. **b** The high *ANLN* expression group had significantly lower disease-free

survival. $P = 0.01$. **c** The relation between the pathological grade of BC and *ANLN* expression. The high-grade BC group shows higher *ANLN* expression. *, $P < 0.0001$. **d** Immunohistochemical staining of ANLN and Ki67 in BC specimens

strategy is reliable. Interestingly, overexpression of *E2F1*, a master transcriptional factor contributed to MIBC progression and its expression was significantly associated with *EZH2* and *SUZ12* expression [43, 44]. Moreover, overexpression of *E2F1/EZH2/SUZ2* enhanced cancer cell migration, invasion, and colony formation [43, 44]. From these things, screening for *miR-223-3p* or *miR-223-5p* targets could provide effective information for BC treatment.

To elucidate the involvement of both *miR-223-5p* and *miR-223-3p* in BC pathogenesis, we analyzed the molecular targets regulated by these molecules. In the present study, we identified 20 putative target genes regulated by *miR-223-3p* (the guide strand) and 26 by *miR-223-5p* (the passenger strand) in BC cells. Among these target genes (46 genes), high-expression levels of 8 genes (*ANLN*, *INHBA*, *OIP5*, *CCNB1*, *CDCA2*, *KIF4A*, *ECT2*, and *RHOB*) were associated with poor prognosis of BC patients. Analysis of

these genes is important for deeper understanding of the molecular pathogenesis of BC. We focused on *ANLN* because its expression was regulated by *miR-223-5p* and its expression was deeply associated with poor prognosis of BC by a large number of cohort analyses.

Based on its sequence, it has been predicted that *ANLN* has multiple functions, such as an actin-binding, myosin-binding, and pleckstrin-homology domains [45]. *ANLN* is localized primarily in the nucleus during interphase; in telophase, it moves to the cytoplasm and forms the contractile ring and cleavage furrow [46]. Overexpression of *ANLN* enhances the metastatic potential of several types of cancer cells, including lung, breast, and colon cancers [47–49]. Recent study of pancreatic adenocarcinoma (PDAC) showed that knockdown of *ANLN* significantly inhibited cancer cell migration and invasion [50]. Moreover, Kaplan–Meier survival curves showed that high expression

of *ANLN* predicted shorter survival of patients with PDAC based on TCGA dataset analysis [50]. More recently, *ANLN* was identified as a frequently overexpressed gene in BC by RNA sequencing and its expression is a promising prognostic biomarker in this disease [51]. These studies and our present data showed that aberrantly expressed *ANLN* acted as a pivotal player for BC cell aggressiveness and metastasis [51]. Exploration of novel anti-tumor *miR-233-5p*-mediated pathways may lead to the development of new treatment protocols for this disease. Previous studies indicated that expression of *ANLN* was directly regulated by *miR-217* and *miR-497* in pancreatic cancer and nasopharyngeal carcinoma, respectively [50, 52]. It would be necessary to investigate the involvement of these miRNAs in BC pathogenesis.

In conclusion, both strands of the *miR-223*-duplex, *miR-223-5p* (the passenger strand), and *miR-223-3p* (the guide strand), acted as anti-tumor miRNAs through their targeting of several oncogenic genes in BC cells. *ANLN*, a gene encoding a multifunctional actin-binding protein was directly regulated by *miR-223-5p*. Overexpression of *ANLN* was involved in the pathogenesis of BC and acted as an oncogene. The anti-tumor function of the passenger strand of miRNA is a new concept in cancer research and searching for molecular mechanisms controlled by passenger strands of miRNA is a new challenge in studies of BC pathogenesis.

Acknowledgements This study was supported by KAKENHI grants 17K16778(B), 17K16777(B), 16K20125(B), 17K11160(C), 16H05462(B), and 15K10801(C).

Compliance with ethical standards

Conflict of interest The authors declare that they have no conflict of interest.

References

1. Antoni S, Ferlay J, Soerjomataram I, Znaor A, Jemal A, Bray F. Bladder cancer incidence and mortality: a global overview and recent trends. *Eur Urol*. 2017;71:96–108.
2. Siegel RL, Miller KD, Jemal A. Cancer statistics, 2015. *CA Cancer J Clin*. 2015;65:5–29.
3. Aldousari S, Kassouf W. Update on the management of non-muscle invasive bladder cancer. *Can Urol Assoc J*. 2010;4:56–64.
4. Veeratterapillay R, Heer R, Johnson MI, Persad R, Bach C. High-risk non-muscle-invasive bladder cancer-therapy options during intravesical BCG shortage. *Curr Urol Rep*. 2016;17:68.
5. Meeks JJ, Bellmunt J, Bochner BH, Clarke NW, Daneshmand S, Galsky MD, et al. A systematic review of neoadjuvant and adjuvant chemotherapy for muscle-invasive bladder cancer. *Eur Urol*. 2012;62:523–33.
6. DeGeorge KC, Holt HR, Hodges SC. Bladder cancer: diagnosis and treatment. *Am Fam Physician*. 2017;96:507–14.
7. Bartel DP. MicroRNAs: genomics, biogenesis, mechanism, and function. *Cell*. 2004;116:281–97.
8. Filipowicz W, Bhattacharyya SN, Sonenberg N. Mechanisms of post-transcriptional regulation by microRNAs: are the answers in sight? *Nat Rev Genet*. 2008;9:102–14.
9. Friedman RC, Farh KKH, Burge CB, Bartel DP. Most mammalian mRNAs are conserved targets of microRNAs. *Genome Res*. 2009;19:92–105.
10. Kong YW, Ferland-McCollough D, Jackson TJ, Bushell M. microRNAs in cancer management. *Lancet Oncol*. 2012;13:e249–258.
11. Koshizuka K, Hanazawa T, Arai T, Okato A, Kikkawa N, Seki N. Involvement of aberrantly expressed microRNAs in the pathogenesis of head and neck squamous cell carcinoma. *Cancer Metastasis Rev*. 2017;36:525–45.
12. Yonemori K, Kurahara H, Maemura K, Natsugoe S. MicroRNA in pancreatic cancer. *J Hum Genet*. 2017;62:33–40.
13. Kita Y, Yonemori K, Osako Y, Baba K, Mori S, Maemura K, et al. Noncoding RNA and colorectal cancer: its epigenetic role. *J Hum Genet*. 2017;62:41–47.
14. Kurozumi S, Yamaguchi Y, Kurozumi M, Ohira M, Matsumoto H, Horiguchi J. Recent trends in microRNA research into breast cancer with particular focus on the associations between microRNAs and intrinsic subtypes. *J Hum Genet*. 2017;62:15–24.
15. Koshizuka K, Hanazawa T, Fukumoto I, Kikkawa N, Okamoto Y, Seki N. The microRNA signatures: aberrantly expressed microRNAs in head and neck squamous cell carcinoma. *J Hum Genet*. 2017;62:3–13.
16. Hobert O. Gene regulation by transcription factors and microRNAs. *Science*. 2008;319:1785–6.
17. Itesako T, Seki N, Yoshino H, Chiyomaru T, Yamasaki T, Hidaka H, et al. The microRNA expression signature of bladder cancer by deep sequencing: the functional significance of the miR-195/497 cluster. *PLoS ONE*. 2014;9:e84311.
18. Yonemori M, Seki N, Yoshino H, Matsushita R, Miyamoto K, Nakagawa M, et al. Dual tumor-suppressors miR-139-5p and miR-139-3p targeting matrix metalloproteinase 11 in bladder cancer. *Cancer Sci*. 2016;107:1233–42.
19. Matsushita R, Yoshino H, Enokida H, Goto Y, Miyamoto K, Yonemori M, et al. Regulation of UHRF1 by dual-strand tumor-suppressor microRNA-145 (miR-145-5p and miR-145-3p): Inhibition of bladder cancer cell aggressiveness. *Oncotarget*. 2016;7:28460–87.
20. Chendrimada TP, Gregory RI, Kumaraswamy E, Norman J, Cooch N, Nishikura K, et al. TRBP recruits the Dicer complex to Ago2 for microRNA processing and gene silencing. *Nature*. 2005;436:740–4.
21. Bartel DP. MicroRNAs: target recognition and regulatory functions. *Cell*. 2009;136:215–33.
22. Koshizuka K, Nohata N, Hanazawa T, Kikkawa N, Arai T, Okato A, et al. Deep sequencing-based microRNA expression signatures in head and neck squamous cell carcinoma: dual strands of pre-miR-150 as antitumor miRNAs. *Oncotarget*. 2017;8:30288–304.
23. Goto Y, Kurozumi A, Arai T, Nohata N, Kojima S, Okato A, et al. Impact of novel miR-145-3p regulatory networks on survival in patients with castration-resistant prostate cancer. *Br J Cancer*. 2017;117:409–20.
24. Yonemori K, Seki N, Idichi T, Kurahara H, Osako Y, Koshizuka K, et al. The microRNA expression signature of pancreatic ductal adenocarcinoma by RNA sequencing: anti-tumour functions of the microRNA-216 cluster. *Oncotarget*. 2017;8:70097–115.
25. Matsushita R, Seki N, Chiyomaru T, Inoguchi S, Ishihara T, Goto Y, et al. Tumour-suppressive microRNA-144-5p directly targets CCNE1/2 as potential prognostic markers in bladder cancer. *Br J Cancer*. 2015;113:282–9.
26. Arai T, Okato A, Kojima S, Idichi T, Koshizuka K, Kurozumi A, et al. Regulation of spindle and kinetochore-associated protein 1

- by antitumor miR-10a-5p in renal cell carcinoma. *Cancer Sci*. 2017;108:2088–101.
27. Yamada Y, Nishikawa R, Kato M, Okato A, Arai T, Kojima S, et al. Regulation of HMGB3 by antitumor miR-205-5p inhibits cancer cell aggressiveness and is involved in prostate cancer pathogenesis. *J Hum Genet*. 2018;63:195–205.
 28. Okato A, Arai T, Yamada Y, Sugawara S, Koshizuka K, Fujimura L, et al. Dual strands of pre-miR-149 inhibit cancer cell migration and invasion through targeting FOXM1 in renal cell carcinoma. *Int J Mol Sci*. 2017;18:E1969.
 29. Fukumoto I, Hanazawa T, Kinoshita T, Kikkawa N, Koshizuka K, Goto Y, et al. MicroRNA expression signature of oral squamous cell carcinoma: functional role of microRNA-26a/b in the modulation of novel cancer pathways. *Br J Cancer*. 2015;112:891–900.
 30. Mah SM, Buske C, Humphries RK, Kuchenbauer F. miRNA*: a passenger stranded in RNA-induced silencing complex? *Crit Rev Eukaryot Gene Expr*. 2010;20:141–8.
 31. Mataka H, Seki N, Mizuno K, Nohata N, Kamikawaji K, Kumamoto T, et al. Dual-strand tumor-suppressor microRNA-145 (miR-145-5p and miR-145-3p) coordinately targeted MTDH in lung squamous cell carcinoma. *Oncotarget*. 2016;7:72084–98.
 32. Yamada Y, Koshizuka K, Hanazawa T, Kikkawa N, Okato A, Idichi T, et al. Passenger strand of miR-145-3p acts as a tumor-suppressor by targeting MYO1B in head and neck squamous cell carcinoma. *Int J Oncol*. 2018;52:166–78.
 33. Pinatel EM, Orso F, Penna E, Cimino D, Elia AR, Circosta P, et al. miR-223 is a coordinator of breast cancer progression as revealed by bioinformatics predictions. *PLoS ONE*. 2014;9:e84859.
 34. Tang Y, Wang Y, Chen Q, Qiu N, Zhao Y, You X. MiR-223 inhibited cell metastasis of human cervical cancer by modulating epithelial-mesenchymal transition. *Int J Clin Exp Pathol*. 2015;8:11224–9.
 35. Gao Y, Lin L, Li T, Yang J, Wei Y. The role of miRNA-223 in cancer: function, diagnosis and therapy. *Gene*. 2017;616:1–7.
 36. Kurozumi A, Goto Y, Matsushita R, Fukumoto I, Kato M, Nishikawa R, et al. Tumor-suppressive microRNA-223 inhibits cancer cell migration and invasion by targeting ITGA3/ITGB1 signaling in prostate cancer. *Cancer Sci*. 2016;107:84–94.
 37. Aziz F. The emerging role of miR-223 as novel potential diagnostic and therapeutic target for inflammatory disorders. *Cell Immunol*. 2016;303:1–6.
 38. Haneklaus M, Gerlic M, O'Neill LA, Masters SL. miR-223: infection, inflammation and cancer. *J Intern Med*. 2013;274:215–26.
 39. Zeng Y, Zhang X, Kang K, Chen J, Wu Z, Huang J, et al. MicroRNA-223 attenuates hypoxia-induced vascular remodeling by targeting RhoB/MLC2 in pulmonary arterial smooth muscle cells. *Sci Rep*. 2016;6:24900.
 40. Huang BS, Luo QZ, Han Y, Huang D, Tang QP, Wu LX. MiR-223/PAX6 axis regulates glioblastoma stem cell proliferation and the chemo resistance to TMZ via regulating PI3K/Akt pathway. *J Cell Biochem*. 2017;118:3452–61.
 41. Arts FA, Keogh L, Smyth P, O'Toole S, Ta R, Gleeson N, et al. miR-223 potentially targets SWI/SNF complex protein SMARCD1 in atypical proliferative serous tumor and high-grade ovarian serous carcinoma. *Hum Pathol*. 2017;70:98–104.
 42. Zhou K, Feng X, Wang Y, Liu Y, Tian L, Zuo W, et al. miR-223 is repressed and correlates with inferior clinical features in mantle cell lymphoma through targeting SOX11. *Exp Hematol*. 2018;58:27–34.e21.
 43. Lee JS, Leem SH, Lee SY, Kim SC, Park ES, Kim SB, et al. Expression signature of E2F1 and its associated genes predict superficial to invasive progression of bladder tumors. *J Clin Oncol*. 2010;28:2660–7.
 44. Lee SR, Roh YG, Kim SK, Lee JS, Seol SY, Lee HH, et al. Activation of EZH2 and SUZ12 regulated by E2F1 predicts the disease progression and aggressive characteristics of bladder cancer. *Clin Cancer Res*. 2015;21:5391–403.
 45. Oegema K, Savoian MS, Mitchison TJ, Field CM. Functional analysis of a human homologue of the *Drosophila* actin binding protein anillin suggests a role in cytokinesis. *J Cell Biol*. 2000;150:539–52.
 46. Giansanti MG, Bonaccorsi S, Gatti M. The role of anillin in meiotic cytokinesis of *Drosophila* males. *J Cell Sci*. 1999;112(Pt 14):2323–34.
 47. Suzuki C, Daigo Y, Ishikawa N, Kato T, Hayama S, Ito T, et al. ANLN plays a critical role in human lung carcinogenesis through the activation of RHOA and by involvement in the phosphoinositide 3-kinase/AKT pathway. *Cancer Res*. 2005;65:11314–25.
 48. Wang Z, Chen J, Zhong MZ, Huang J, Hu YP, Feng DY, et al. Overexpression of ANLN contributed to poor prognosis of anthracycline-based chemotherapy in breast cancer patients. *Cancer Chemother Pharmacol*. 2017;79:535–43.
 49. Wang G, Shen W, Cui L, Chen W, Hu X, Fu J. Overexpression of Anillin (ANLN) is correlated with colorectal cancer progression and poor prognosis. *Cancer Biomark*. 2016;16:459–65.
 50. Idichi T, Seki N, Kurahara H, Yonemori K, Osako Y, Arai T, et al. Regulation of actin-binding protein ANLN by antitumor miR-217 inhibits cancer cell aggressiveness in pancreatic ductal adenocarcinoma. *Oncotarget*. 2017;8:53180–93.
 51. Zeng S, Yu X, Ma C, Song R, Zhang Z, Zi X, et al. Transcriptome sequencing identifies ANLN as a promising prognostic biomarker in bladder urothelial carcinoma. *Sci Rep*. 2017;7:3151.
 52. Wang S, Mo Y, Midorikawa K, Zhang Z, Huang G, Ma N, et al. The potent tumor suppressor miR-497 inhibits cancer phenotypes in nasopharyngeal carcinoma by targeting ANLN and HSPA4L. *Oncotarget*. 2015;6:35893–907.